(article starts on next page)

Ultimate limit state analysis of a double-hull tanker subjected to biaxial bending in intact and collision-damaged conditions

Artjoms Kuznecovs [a], Jonas W. Ringsberg [a,*], Erland Johnson [a,b], Yasuhira Yamada [c]

[a] *Chalmers University of Technology, Department of Mechanics and Maritime Sciences, Division of Marine Technology, SE-412 96, Gothenburg, Sweden*
[b] *RISE Research Institutes of Sweden, Department of Applied Mechanics, P.O. Box 857, SE-501 15, Borås, Sweden*
[c] *National Institute of Maritime, Port and Aviation Technology, Structural Strength Evaluation Department, Tokyo, 181-0004, Japan*

ABSTRACT

This study presents a comparison between nonlinear finite element analysis (FEA) and the Smith method of Fujikubo et al. (2012). The objective was to compare the accuracy and computation effort of the two methods for a double-hull tanker under biaxial bending and various ship conditions: intact hull structure, collision-damaged hull structure, newly built condition, and ship hull aged due to corrosion. The results for the non-corroded and intact ship hull structures showed good agreement between FEA, the Smith method and IACS CSR-H for vertical bending loading conditions. For all other bending load combinations, FEA always gave lower ultimate bending moments than the Smith method. The differences between the two methods were larger for the corroded and damaged ship hull structure than for other conditions. Results from ultimate strength analyses of the collision-damaged hull structures showed that both methods captured the expected asymmetric ultimate strength response due to asymmetric damage. A residual strength index calculation showed that the reduction was larger for the FEA than for the Smith method. A procedure is proposed that combines results of a few FEAs with the advantages of the Smith method to generate accurate biaxial bending load interaction curves for different ship conditions.

1. Introduction

After several ship accidents following the loss of the ship Prestige, the concept of an ultimate residual strength of the hull girder was introduced to the IMO Goal Based Ship Construction Standards (IMO-GBS) as a new SOLAS convention at the 87th session of the Maritime Safety Committee in IMO (IMO, 2010; Yamada and Ogawa, 2011). The IMO-GBS is currently applied to all tankers and bulk carriers 150 m in length or longer. It is also required for large container ships and for other ships. Residual strength is a functional requirement included in Tier II of IMO-GBS and is defined in IMO (2010) as follows: "II.5 Residual strength – Ships shall be designed to have sufficient strength to withstand the wave and internal loads in specified damaged conditions such as collision, grounding or flooding. Residual strength calculations shall take into account the ultimate reserve capacity of the hull girder, including permanent deformation and post-buckling behaviour. Actual foreseeable scenarios shall be investigated in this regard as far as is reasonably practicable."

The ultimate limit state (ULS) of a ship structure is the instant of the peak design load at which the ship structure collapses due to loss of its structural stiffness and strength (Paik, 2018). This point is defined as the ultimate strength, and it is of paramount importance for safe ship design to know the ULS with regard to all loads and the loading conditions a ship will be subjected to during its operational life. Ultimate and residual strength calculations of ship structures can be carried out using several methods. Finite element analysis (FEA) is becoming more and more common procedure even though it requires significant modelling and computation efforts. The simplified method proposed by Smith (1977) and further developed by many researchers, such as Fujikubo et al. (2012), has been approved by classification societies and is one of the accepted simplified numerical procedures in the Harmonised Common Structural Rules for oil tankers and bulk carriers (CSR-H) (IACS, 2019). Czujko et al. (2018) discussed pros and cons of other well-known methods for ultimate and residual strength calculations such as the Panel Ultimate Limit State (PULS) method, the Intelligent Supersize FE Method (ISFEM) and the Idealised Structural Unit Method (ISUM).

ULS analysis of ship structures can be categorised into studies or combinations of studies of intact or damaged ship structures that have different physical conditions due to corrosion or fatigue cracks. In this work, damaged and intact hulls refer to hulls with and without

---

structural damage due to accidents such as collision and grounding, respectively. Finite element models for ultimate and ship collision analyses can be made highly detailed and realistic for the scenarios they are designed to simulate. Although this enables the thorough analyses of specific cases with regards to structural integrity and failures, the computational cost and effort for each case are high. From a modelling and computational effort perspective, the Smith method, for example, requires significantly less computational time than FEA. The Smith method is accepted by classification societies for ultimate and residual strength assessments since it, in contrast to FEA, yields results relatively fast and with an "accepted accuracy" at a low computational cost. However, FEA and the Smith method should be complementary to ensure that model assumptions and simplifications are made correctly with regards to the predicted ULS level, location and sequence of structural failures preceding the ultimate state.

For pure vertical and horizontal bending conditions, recent studies (e.g. Parunov et al., 2018) show that there is often good agreement between the results of FEA and the Smith method for ships that have no structural damage in the side shell or the bottom caused by collision or grounding, respectively. However, there are studies that have shown that the agreement between FEA and the Smith method is not as good under biaxial bending load conditions (Czujko et al., 2018; Parunov et al., 2018). Even though the ultimate strength of an intact ship structure is often the lowest in pure hogging or sagging conditions, it is important to have knowledge about the ship's ULS characteristics for biaxial bending conditions if the ship has side-shell hull damage from a collision accident. This justifies the need for methods and model developments offering faster and more accurate numerical procedures for the calculation of biaxial bending load interaction diagrams that present the ULS of intact and damaged ship structures, as well as for different physical conditions related to ship age.

Intuitively, a ship structure damaged due to collision will suffer from a reduction in its ultimate and residual strengths. This type of damage is asymmetric with regard to the cross-section of the vessel. The damage is defined by the shape and size of the material rupture and large plastic deformations of the surrounding structural details. To reliably estimate a ship's reserve strength, a ULS analysis of a damaged ship requires descriptions of several issues, e.g., (i) the collision location, (ii) the shape and size of the damage, (iii) the severity of the large plastic deformation of the damaged surrounding material, and (iv) the ship's physical condition due to corrosion. Considerable research efforts have been spent on the structural response during collision and on the residual ultimate strength of struck ships. Examples of such investigations with the representation of materials and their characteristics can be found in Abu-Bakar and Dow (2013), Ehlers (2010), Ehlers and Østby (2012), Hogström and Ringsberg (2012), Hogström et al. (2009), Hussein and Soares (2009), Marinatos and Samuelides (2015), Samuelides (2015), Storheim et al. (2015), Yamada (2014), Yamada and Ogawa (2011), Zhang and Pedersen (2017) and Faisal et al. (2016). Simplified shapes of the structural damages were mainly used in the studies.

A ship's physical condition, which is affected by factors such as corrosion, has a significant impact on the ultimate and residual strength of the ship under both intact and collision-damaged conditions. The IACS regulation of CSR-H requires 50% corrosion reduction according to the rules when evaluating the ultimate and residual strength. Campanile et al. (2015) present a study on the same topic and type of damage for bulk carriers; this study includes the effect of corrosion using a corrosion model proposed by Paik et al. (2003b). The results show how the influence of corrosion of the material leads to a significant decrease in the residual ultimate strength index (RSI). There are several investigations on the buckling ultimate strength that support this finding for intact structures suffering from either minor or major corrosion wastage; see, e.g., Paik et al. (2008a) and Saad-Eldeen et al. (2011). However, there are few studies in the literature that systematically present the consequences of corrosion on the collision resistance and the ultimate strength together. The influence of corrosion is typically simplified by removing

the extra corrosion margin in damage assessments; see Ringsberg et al. (2017) and Parunov et al. (2018).

1.1. Objective of the study

This investigation presents a comparison of methods, i.e., advanced nonlinear FEAs and the Smith method modified by Fujikubo et al. (2012), in the calculation of the ultimate and residual strengths of a double-hull tanker. The objective is to compare the two analysis methods during biaxial bending conditions with regard to their accuracy and computation effort for various ship conditions, such as an intact hull structure, a collision-damaged hull structure, the newly built condition and a physical condition in which the ship hull is aged due to corrosion. A sensitivity study is presented on how the modelling of the damage shape and size, plastic deformation due to collision and simplified material properties affects the ultimate strength calculation using FEA and the Smith method. A method is proposed that shows how the Smith method, after calibration using results from a few FEAs is conducted, can be employed as a reliable and accurate method to compute the ULS of a ship structure during biaxial bending load conditions for intact or damaged ship hull structures, including the ship's physical condition.

1.2. Case study vessel and analyses

The case study vessel is a coastal oil tanker with a deadweight of 11,500 t and draft of 7.4 m. The tanker has a longitudinally stiffened double bottom and weather deck, while the double side-shell structure is transversely stiffened; see Fig. 1 for the mid-ship section of the vessel. The tanker has been used as a case study vessel in previous research by the authors, and readers are referred to Ringsberg et al. (2018a, 2018b) for a more detailed description of the vessel.

Ships of this type and size are common along the west coast of Sweden, where ship traffic density is high and there are crossing ship traffic and fairways between Denmark and Sweden. Concerns of negative environmental consequences in the case of ship collision accidents and the risk of ship loss have been raised. Hence, the ultimate and residual strengths of this type of ship are relevant for studying both intact and collision-damaged conditions. The strength capacity of the ship structure must also be known for biaxial bending conditions to account for arbitrary wave encounter loading conditions, especially for damaged
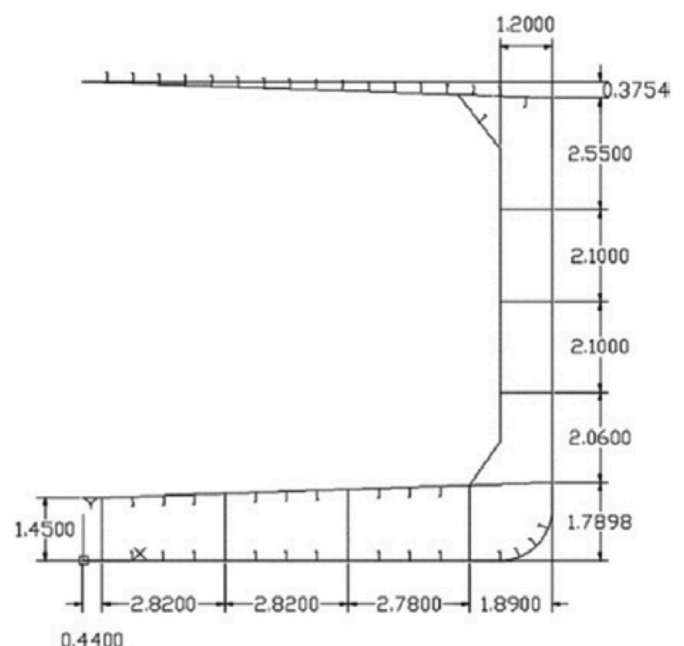

Fig. 1. Mid-ship section of the studied coastal oil tanker (unit: metres).

ship structures. The sensitivity of the calculated ultimate strength capacity of the ship due to its physical condition is also an important factor that can be investigated by comparing the properties of newly built ships and ships aged due to corrosion.

Table 1 presents an overview of combinations of analyses presented in the study. For the simulation cases in which the tanker ship is intact (i. e., free from hull damage from a collision), the FE model in Subsection 2.1 is used only in the biaxial ultimate strength simulations outlined in Subsection 2.2. However, for the simulation cases in which the tanker ship has damage due to collision, the damage is first introduced to the ship, and then the biaxial bending moment load is simulated according to Subsections 2.1 and 2.2, respectively. The Smith method used for progressive collapse analyses and the models are presented in Section 3. The results of the simulations and analyses are presented in Section 4. Finally, in Section 5, the conclusions and recommendations for future research are presented.

2. Finite element models and analyses

This section presents the FE models and analyses for the ship collision and ultimate strength analyses. The FE models and analyses were carried out using Abaqus/Explicit version 6.13-3 (Dassault Systèmes, 2020). A thorough description of the design of the FE models for collision simulation, material characteristics and damage modelling can be found in previous work by the authors; see Hogström and Ringsberg (2012, 2013) and Ringsberg et al. (2017, 2018a). Hence, only a brief summary of these concepts with all necessary information for the reproduction of the collision simulations is presented in Subsection 2.1. Subsection 2.2 presents the FE model of the case study ship subjected to biaxial bending and the related modelling details.

2.1. Ship collision simulations

The collision scenario was a collision between two similar-sized vessels. The struck ship was the case study coastal oil tanker shown in Fig. 1, and the striking ship was a coastal product/chemical tanker with a total displacement of 10,800 t henceforth referred to as the striking tanker. Fig. 2 presents the geometry of the inner structure of the bulbous bow section of the striking tanker and the geometry of the struck coastal oil tanker.

The FE model of the struck ship was made sufficiently large to avoid influence from the boundary conditions. The collision impact was amidships and between bulkheads and web frames (see Fig. 3a). The bow section of the striking tanker was modelled as deformable and restricted to only move in a prescribed right-angle collision direction; other collision angles have already been investigated by Ringsberg et al. (2017). The striking ship was given different initial forward velocities corresponding to different kinetic energies; see Section 4. The velocity of the striking bow gradually decreased to zero knots during the collision event as energy was dissipated through deformations, fractures and friction in the structures. All nodes at the fore and aft faces of the struck ship hull were connected to control points (CP) through a multipoint constraint with a rigid beam connection. This configuration of boundary conditions allowed us to constrain the displacements and rotations in each slave node to the displacements and rotations of the CP. The CPs were placed on the intersection of the centre plane and on the initial elastic neutral axis, and they were fixed in all degrees of freedom during the collision simulations (see Fig. 3b).

The FE meshes were made of four-node shell elements with reduced integration (S4R and some three-node S3R in Abaqus/Explicit) and five section points through the thickness. A mesh convergence analysis of the struck tanker resulted in an element size of 60 mm. The element length/thickness ratio was 5 in the part of the model with the largest sheet thickness. Time step in the explicit analysis was determined automatically. The general contact condition in Abaqus/Explicit was used in conjunction with a friction coefficient of 0.3 (non-corroded surface) or 0.5 (corroded surface); see Section 4 to model the contacts between surfaces in the collision.

In addition to the net cross-section area loss, two factors that have a large impact on strength reduction are, according to Garbatov et al. (2016), the change in material parameters caused by corrosion and the stress concentration due to local corrosion pits. Several investigations in the literature have studied how the strength of corroded metal structures depends on factors such as the degree of degradation, geometric modelling of pit density and initial imperfections in simulation models used in nonlinear FE analysis; see, e.g., Paik et al. (2008b) and Paik and Melchers (2008). In the current study, an approach presented in Ringsberg et al. (2018a) was adopted. Three different representations of NVA shipbuilding mild steel were used depending on the grade of corrosion (ship age and severity of corrosion): NVA virgin (non-corroded), NVA minorly corroded and NVA severely corroded. A detailed description of the material models used in this study is presented in Ringsberg et al. (2018a), and only a brief summary is given below.

The material parameters for the three materials are summarised in Table 2. The NVA virgin material was represented by a nonlinear elastic-plastic power law constitutive material model with isotropic hardening. The influence from the strain rate was considered using the Cowper-Symonds relationship, including the two constants C and P. Degradation leading to failure was modelled using one model for onset of failure based on the shear criterion in Abaqus/Explicit (damage initiation, DI) and one model for material degradation (damage evolution, DE). In the DE model, the length dependence between element size and fracture strain was accounted for through Barba's law; see Hogström et al. (2009) for details.

For the corroded ship structure, the degree of corrosion was considered by simply varying the parameters in the stress-strain law, the structural thickness and the coefficient of friction, a process that can easily be implemented in the FEA; see Ringsberg et al. (2018a). The corroded material was represented by a bilinear elastic-plastic constitutive material model, with linear isotropic hardening between the yield and ultimate tensile stresses. As found in Garbatov et al. (2014), a corroded material is less ductile than a non-corroded material, and the necking point is not easily observed during tensile tests. Hence, the damage model of the corroded materials was represented solely by the shear failure DI criterion without any DE law. Due to the lack of material data for the corroded materials, a sensitivity study was carried out in Ringsberg et al. (2017). The influence of considering a Cowper-Symonds model and a simplified DE model (activated after reaching the fracture strain) was investigated. The results showed that both issues had only a minor influence on the size of the damage opening in the corroded ship structure compared to analyses including no strain rate dependence or DE model. Hence, no Cowper-Symonds or DE models were included in the FEA with corroded material properties; see Ringsberg et al. (2018a).

The corrosion margins of the struck coastal oil tanker, estimated from the Common Structural Rules for Bulk Carriers and Oil Tankers (CSR-BC&OT) (IACS, 2019), are shown in Fig. 4a. Full reduction of a corrosion margin could represent 25 years of operation for a vessel and a 50% reduction in the corrosion margin after approximately 16 years of

Table 1
Overview of combinations of analyses presented in the study. Note: ultimate strength analysis implies that residual strength calculations have also been made.

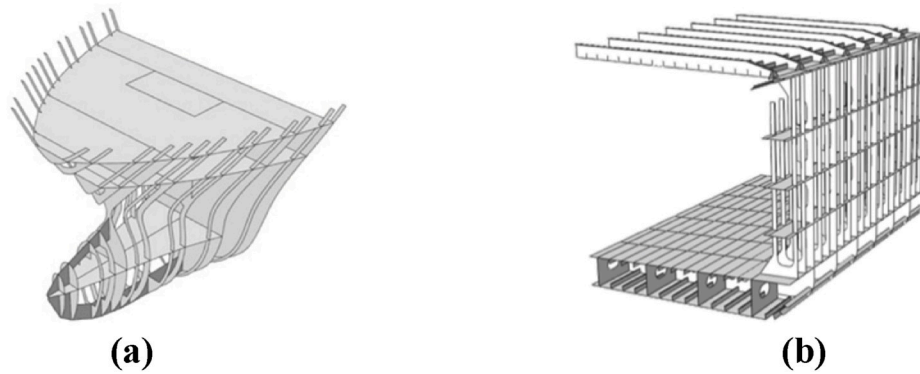| Case study vessel	Initial hull condition	Physical condition	FEA – ship collision	FEA – ultimate strength	Smith method – ultimate strength
T1I	Intact	New		X	X
T5I	Intact	Corroded		X	X
T1D	Damaged	New	X	X	X
T5D	Damaged	Corroded	X	X	X

Fig. 2. The geometry of the inner structure of **(a)** the bulbous bow section of the striking tanker and **(b)** the struck coastal oil tanker.

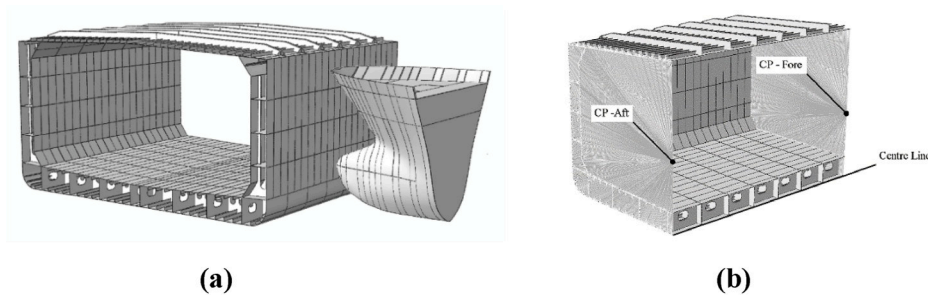**Fig. 3.** **(a)** Definition of collision scenario with positioning of the two vessels. Note that the bulb hits the bilge area and the forecastle on the sheer strake. **(b)** Constrained FE model of the struck vessel showing the CPs.

Table 2
Material parameters used in the constitutive material and damage models from [Ringsberg et al. (2018a)](#).

| Parameter	NVA virgin (non-corroded)	NVA minorly corroded	NVA severely corroded
Young's modulus, E (GPa)	210	179	158
Poisson's ratio, υ (-)	0.3	0.3	0.3
(Static) Yield stress, $\sigma_{y,s}$ (MPa)	310	310	291
Ultimate tensile strength (MPa)	579	518	440
Hardening coefficient, K (MPa)	616	845	752
Hardening exponent, n	0.23	1.00	1.00
Necking strain, ε_n (%)	23.0	-	-
Fracture strain, ε_f (%)	35.1	24.8	20.0
Cowper-Symonds constant, C (-)	40.4	-	-
Cowper-Symonds constant, P (-)	5	-	-
DE parameters, bilinear model; see Dassault Systèmes (2020) for details.	(0, 0), (0.02, 0.00458), (1, 0.01832)	-	-

operation ([Paik et al., 2003a](#)).

The relationship between intervals of the remaining corrosion margin and their correlation with the material model used in FE analyses was established in [Kuznecovs and Shafieisabet (2017)](#). For plates with 0% reduction of as-built thickness, the NVA virgin (non-corroded) material was recommended, for a 0%–20% reduction, the minorly corroded material was recommended, and for a 20%–40% reduction, the severely corroded material was recommended. These intervals are relevant for coastal oil tankers with different structural parts that have various percentages of loss of material due to corrosion. [Fig. 4](#)b presents where in the ships' cross-section different material properties were used in the simulation models; it was assumed that the physical condition of the corroded case study ship represented 25 years of aging and corrosion.

2.2. Biaxial bending loading simulations

The main loading conditions experienced by a ship structure are bending induced by still water conditions (including cargo weight distribution) and from the waves. If the ship is sailing in head or following seas, the hull girder is normally subjected to vertical bending moment, resulting in pure hogging or sagging moments. However, in case of oblique waves, or a heeling angle resulting from partial flooding or parametric rolling, the loading conditions give rise to biaxial bending moment where the ship is subjected to combined loading of both vertical and horizontal bending moments.

The FE model presented in [Subsection 2.1](#) was used to estimate the ultimate strength capacity of the case study vessel during biaxial loading conditions. To estimate the ultimate strength due to bending moment(s), the FE model was bent in a prescribed direction beyond its ultimate state condition. The applied loading continued beyond the ULS to simulate the progressive collapse of different parts and structural elements due to buckling and plastic deformation. The bending was applied to the FE model through displacement control following a procedure proposed by [Parunov et al. (2018)](#) and [Tekgoz et al. (2018)](#): the bending curvature was increased gradually (linearly) by the rotation of the end planes through controlled rotations of the CPs; see [Fig. 5](#) for a schematic and [Subsection 2.1](#) for a detailed description of how the CPs were defined. To preserve pure bending, one of the CPs was pinned and restricted from translation in three directions, while the other CP was allowed to move in the longitudinal x-direction. By controlling the ratio between the horizontal and vertical rotations, the desired biaxial bending condition was achieved. The applied curvature components were then $\chi_H = 2\varphi_z/L$
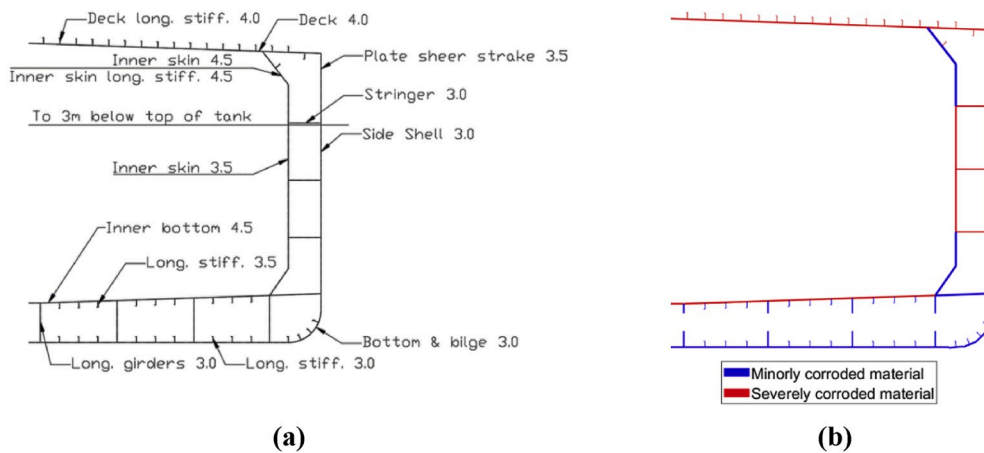
Fig. 4. **(a)** Corrosion margins (unit: mm) and **(b)** different material models used for the corroded ship cases T5I and T5D.
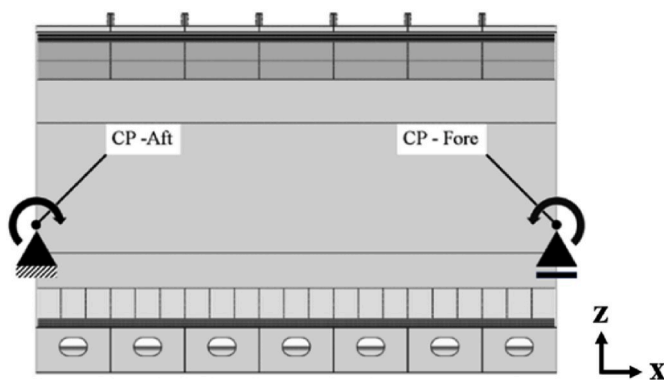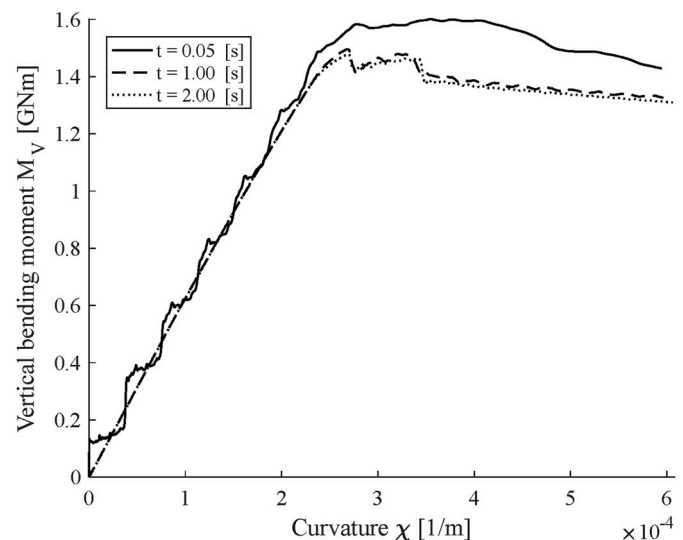

Fig. 5. Illustration of boundary conditions during bending simulations.

Fig. 6. Convergence analysis of the influence of simulation time on the vertical bending moment.

and $\chi_V = 2\varphi_y/L$, where φ_z and φ_y are the applied rotation angles around the z- and y-axes, respectively, and L is the distance between the CPs. The reaction moment at the CPs was recorded for every curvature increment during bending. The maximum point on the obtained total bending moment-total curvature curve defined the ultimate strength as its ULS bending moment and corresponding curvature.

It was shown in Yamada (2014, 2019) that the time duration of loading in explicit FEA can have a significant influence on the ultimate bending moment. Fig. 6 shows a convergence analysis conducted in this study with the intact, non-corroded FE model and presents the vertical bending moment vs applied curvature in hogging for three different loading times. The shortest loading time ($t = 0.05$ s) resulted in structural vibrations due to the sudden loading, which led to an over-estimation of the ultimate bending moment. The longer loading time showed a decrease in this artificial dynamic response. The convergence analysis showed that a loading time of 1.00 s was sufficient for the FE model used in the current investigation.

Initial deformations and imperfections which occur during the manufacturing process of a ship affect its ULS. The presence of initial imperfections will reduce the ultimate strength of a hull due to decreased critical buckling stress of its components. For the double bottom tanker the effect of initial imperfections is more critical in sagging due to the lower buckling strength of the weather deck as compared to the double bottom. Despite this, the majority of studies in the literature that have analysed the ULS using full-ship FE models disregard the influence of these mainly due to the complexity of setting up the simulation model with e.g. initial imperfections. This study did not include initial deformations and imperfections in the FE model for the same reason, which was also supported by the argument that such imperfections were not (and are normally not) incorporated in the FE model used

in the ship collision simulations. Thus, ultimate strength predictions obtained from intact FE models used in this study may be slightly overestimated compared to FE models with initial imperfections.

Notably, the introduction of hull damage in an FE ship model used for ULS analysis can be conducted in different ways. Ringsberg et al. (2018a) proposed first simulating the ship collision event and then continuing with the same FE model in the ultimate strength simulation analysis. Parunov et al. (2018) proposed simplifying the shape and size of the damage opening and removing the corresponding elements in the FE model prior to the ULS analysis. With this simplification, the shape and size of the damage may not be correct, and the plastic deformation and failures of structural elements are disregarded. With the Smith method (see Section 3), similar assumptions and simplifications must be made, and the material must also be elastic-perfectly plastic. Thus, Section 4 presents the results from a sensitivity study on how these different damage modelling perspectives differ and affect the ULS, as well as a discussion on which alternative is the most suitable for the design of safe ships.

3. Smith method and models

In numerical simulations using the FE method, a substantial amount of time and effort is required to prepare the model and to conduct the

simulation. For example, the computation time required to obtain one value of the ultimate bending moment using the undamaged FE model presented in Section 2 is approximately 60 CPU hours on a desktop computer with four core processors working at a base frequency of 3.5 GHz and 32 GB RAM. The computational time and cost are high, but the detailed results and the possibility of investigating different failure modes and post-collapse characteristics justify it for a few FEAs. For the same type of analysis, simplified analysis procedures such as the Smith method (Smith, 1977) are less computationally demanding and much faster than the FE method, requiring less than 1 min per loading case, but have limitations in the type of results that can ultimately be provided.

For the purpose of ULS analysis of the tanker ship in this study, both analysis methods were tested. One of the major advantages of the Smith method is that it provides fast analyses. This option can be beneficial for the rapid assessment of impacts on structural integrity, such as after a collision or grounding accident, or for parametric studies. It also can be implemented as a code in more complex prediction tools to check for the effect of structural ageing or in real-time reliability assessments of ship structure.

In this study, the Smith method further developed by Fujikubo et al. (2012) was implemented in the in-house code used for ULS analyses and was verified against other studies in the literature by Kuznecovs and Shafieisabet (2017). The method was used due its ability to consider the instant translation and rotation of the neutral axis (NA) during bending. The importance of including the NA's two-dimensional movement for correct estimation of the ULS in the case of asymmetric geometry, material distributions or load applications has been studied and discussed by several authors, such as Choung et al. (2012), Makouei et al. (2015), Smith and Pegg (2003) and Tekgoz et al. (2018). The reader is referred to the work by Fujikubo et al. (2012) for a detailed description of the methodology. In the following, only the basics and some minor modifications to the method introduced by the authors are presented.

The Smith method, as proposed by Fujikubo et al. (2012), is a pure incremental seminumerical method for simplified ULS analysis of ships during biaxial bending loading without torsion. The cross-section of the hull is divided into three types of structural elements: stiffened plates, stiffeners and hard corners. In the current work, the longitudinal girders with openings are modelled as two independent stiffened plate elements with a distance between them corresponding to the opening breadth. The average stress responses in the hull's longitudinal direction for every element in the cross-section due to imposed loading are described by load shortening elongation (LSE) curves. These curves can give the material and structure different stiffness properties and characteristics. The LSE curves in the present study were defined by the seminumerical expressions in the CSR-H rules in IACS (2019). As defined in the CSR-H rules, the material in this simplified analysis, in contrast to the more advanced and realistic material models used in an FE model, was modelled as elastic-perfectly plastic. This assumption implies limitations on the post-ultimate behaviour of the ship structure while holding reasonably well in the pre-ultimate and ultimate regions (see further discussion in Section 4). The effect of initial imperfections and residual stresses, e.g., due to welding, were implicitly included in the Smith method through the equations that define the LSE curves according to the CSR-H rules in IACS (2019).

Hull damage caused by a collision event was modelled as a damage opening by removing and adjusting the geometry of the structural elements corresponding to the ruptured and severely plastically deformed elements in the ship's cross-section. LSE curves of the modified elements were adjusted accordingly. The longitudinal location of the representative cross-section was chosen from the FEA of the collision event by identification of the cross-section that had the most extensive damage. Furthermore, the influence of corrosion was determined following the method presented in Subsection 2.2; the reduction in the thickness of structural elements and adjustment of the material properties were made according to Table 2. Note that only the elastic modulus and the

yield stress were changed because the material curve of the Smith method ship model must be represented by an elastic-perfectly plastic curve.

In the Smith method used in this study, the changes in the global reaction forces and moments during bending at every curvature increment were found by integration of the tangential axial stiffness around the instant NA throughout the whole cross-section. If the bending load was applied gradually and the curvature increments were sufficiently small, no iterative procedure was required (Smith, 1977). The change in the global structural response during biaxial bending under the prescribed moment ratio was found by incrementally solving a system of nonlinear equations:

$$\left\{ \begin{array}{c} \alpha \Delta M_V \\ \Delta M_V \end{array} \right\} = \begin{bmatrix} D_{HH} & D_{HV} \\ D_{VH} & D_{VV} \end{bmatrix} \left\{ \begin{array}{c} \Delta \chi_H \\ \Delta \chi_V \end{array} \right\} = D \left\{ \begin{array}{c} \Delta \chi_H \\ \Delta \chi_V \end{array} \right\} \tag{1}$$

where the factor $\alpha = \Delta M_H / \Delta M_V$ is the ratio between the horizontal (M_H) and vertical (M_V) moment components, D is the tangential stiffness matrix and $\Delta \chi_H$ and $\Delta \chi_V$ are the curvatures in the horizontal and vertical directions, respectively. From this definition, it follows that pure horizontal and vertical bending is achieved when $\alpha \to \pm \infty$ and $\alpha = 0$, respectively.

To solve the equation system, one of the curvature step components $\Delta \chi_H$ or $\Delta \chi_V$ should be prescribed. For better numerical convergence, $\Delta \chi_V$ was prescribed when $|\alpha| < 1$, i.e., when the contribution from vertical bending prevailed, while $\Delta \chi_H$ was prescribed when $|\alpha| > 1$. The components of the tangential stiffness matrix D of the cross-section of the ship model for a specified curvature were defined as:

$$D_{VV} = \sum_{i=1}^{N} D_i (z_i - z_G)^2 A_i \tag{2}$$

$$D_{HH} = \sum_{i=1}^{N} D_i (y_i - y_G)^2 A_i \tag{3}$$

$$D_{HV} = D_{VH} = \sum_{i=1}^{N} D_i (y_i - y_G)(z_i - z_G) A_i \tag{4}$$

where A_i is the cross-sectional area of an element, y_i and z_i are the coordinates of an element's centre of mass, and y_G and z_G are the centroid coordinates of the cross-section (see Fig. 7). The tangential stiffness D_i of every i-th element in the cross-section subjected to bending at curvature step j was defined by the slope of the corresponding LSE curve at instant strain. For every curvature increment, the centroid G of the instant NA was found by Equation (5).

$$y_G = \frac{\sum_{i=1}^{N} D_i A_i y_i}{\sum_{i=1}^{N} D_i A_i} z_G = \frac{\sum_{i=1}^{N} D_i A_i z_i}{\sum_{i=1}^{N} D_i A_i} \tag{5}$$

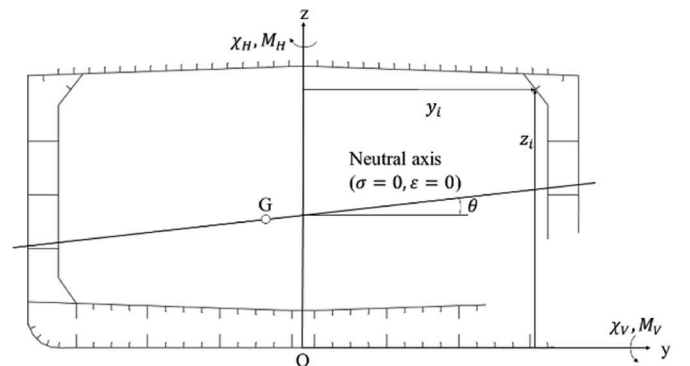The obtained increments of the bending moment and the curvature

Fig. 7. Neutral axis (NA) position, centroid (G) and loading (M_H, M_V) for a cross-section with asymmetric damage.

were added to their cumulative values. By plotting the total bending moment versus the total curvature, the ULS could be identified and defined as the maximum bending moment for the specific loading condition. This was repeated for many combinations of horizontal and vertical bending moments. By plotting their maxima in a biaxial plot, an interaction curve describing the ship's ultimate strength for its specific bending and structural condition was produced for all possible biaxial bending moment combinations. The bending moment load ratios are presented in polar diagrams, which show the bending moment loading ratios in degrees and the ULS values in the radial direction (see Fig. 8). Here, for example, 90° and 270° ($\alpha = 0$) correspond to hogging and sagging, respectively. Pure horizontal bending with the port side in tension occurs at 0°, and compression occurs at 180° ($\alpha \rightarrow \pm \infty$).

4. Results and discussion

This section presents the results from the simulations and analyses in four sections. Subsection 4.1 presents the FEA of ship collision events in which the speed of the striking ship varied. The outcome of these analyses was the target speed of the striking vessel, which served as a representative candidate for the hull damage calculation due to collision used in the ULS analyses in Subsection 4.2. This section also presents a comparison of different alternatives for modelling hull damage and how these affect the ULS predicted by FEA or the Smith method. Subsection 4.3 presents the results from the biaxial bending moment load analyses in which both the ultimate and residual strengths were assessed and compared between FEA and the Smith method. Finally, in Subsection 4.4, a method is proposed that shows how the Smith method, after calibration using results from a few FEAs, becomes a more accurate and reliable method to assess a ship for these conditions.

4.1. FEA of ship collision: shape and size of damage and structural deformation

The damage caused to two ships involved in a collision depends on several factors, such as their relative displacements, the ship speeds, the collision location, the collision angle and the strength of their structures. The schematic in Fig. 9 shows the different principal categories of
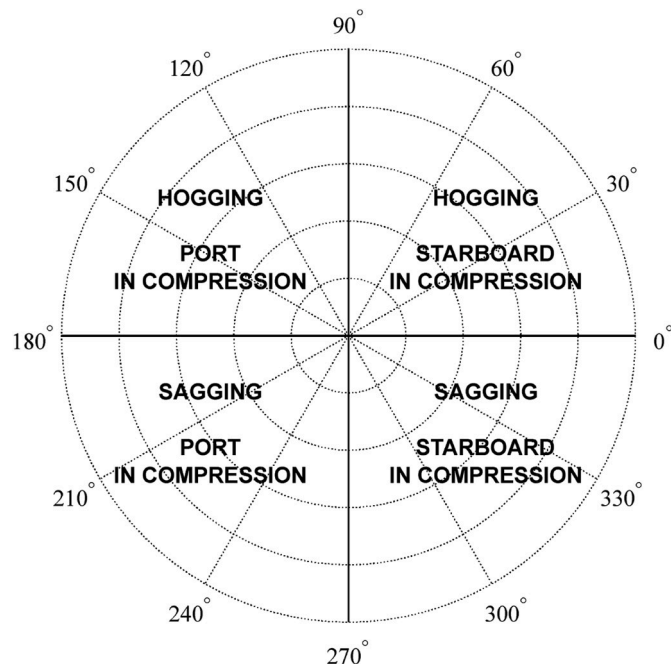
Fig. 8. Definition of ship structure ULS responses and bending moment ratios in a biaxial polar diagram.

damage to a struck ship and their dependence on the relative stiffnesses of the striking and struck ships (NORSOK, 2004).

Subsection 2.1 describes the two ships that were used to simulate the collision event in the current study. The velocity of the struck ship was zero knots, while the velocity of the striking ship was derived from analyses of several ship collision simulations to provide a "realistic" velocity for the ULS analyses. The initial velocity of the striking ship varied from 2 knots to 8 knots with an increment of 1 knot. This was carried out for both the non-corroded struck ship (referred to as "T1") and the corroded struck ship (referred to as "T5"); note that the striking ship was always represented by a non-corroded ship model.

The results are presented in Fig. 10 as the relative energies shared between frictional dissipation, internal energy in the striking ship (bow) and the struck ship (hull). For the non-corroded T1 cases, the strength of the struck ship was large enough to deform the bow of the striking ship. At low collision speeds, more internal energy was dissipated in the struck ship because the penetration depth of the struck ship hardly reached the inner structure. The share of the internal energies was more equal at high collision speeds because of the large penetration depth, which resulted in large contact between the bow and side-shell structure; it also forced the forecastle to have a large amount of plastic deformation. For the T5 cases, the struck ship took the most internal energy because the strength of the structure was weakened due to the loss of corrosion margin and change in material properties. The bow was still deformed at the highest collision speeds, while it remained almost undeformed at the lowest collision speeds. Frictional dissipation was larger for T5 than for T1 due to the higher friction coefficient in the contact between surfaces.

The results in Fig. 10 show that the structural deformation and energy dissipation according to Fig. 9 probably corresponded to the shared-energy design for T1 and ductile design for T5. By calculating the relative internal energy share ratio for the struck ship, $R_{IE,struck}$, according to Equation (6), it was confirmed in Fig. 11a that this was true for T1 and for T5, except for when the ship speed was 5 knots. In this case, the results were more or less on the border line between the shared-energy and ductile designs. Fig. 11b presents the projected damaged areas of the inner and outer side-shells. The results show that for T5 at 5 knots, there was a drastic increase in the damage opening area. Because of these results, 5 knots was chosen as the reference collision velocity for the striking ship in the collision scenario and is also a speed often used in similar types of ship collision studies.

$$R_{IE,struck} = IE_{struck} / \left(IE_{striking} + IE_{struck} \right) \cdot 100\% \qquad (6)$$

4.2. Comparison of FEA and Smith method – selected cases

4.2.1. Intact ship structure

The results from the FEA of the intact ship structure with new (non-corroded) material were compared against analyses using a Smith method model for the bending moment load directions 0, 60, 90 and
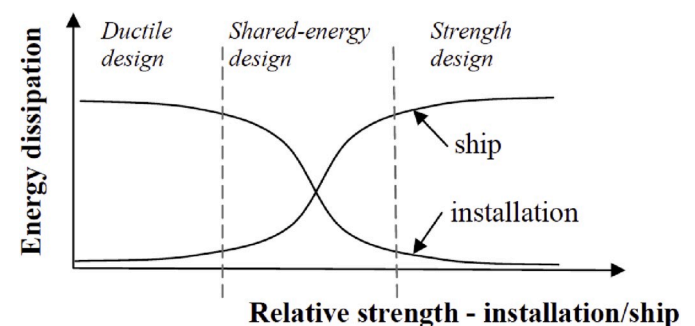
Fig. 9. Energy dissipation for strength, ductile and shared-energy designs (NORSOK, 2004).
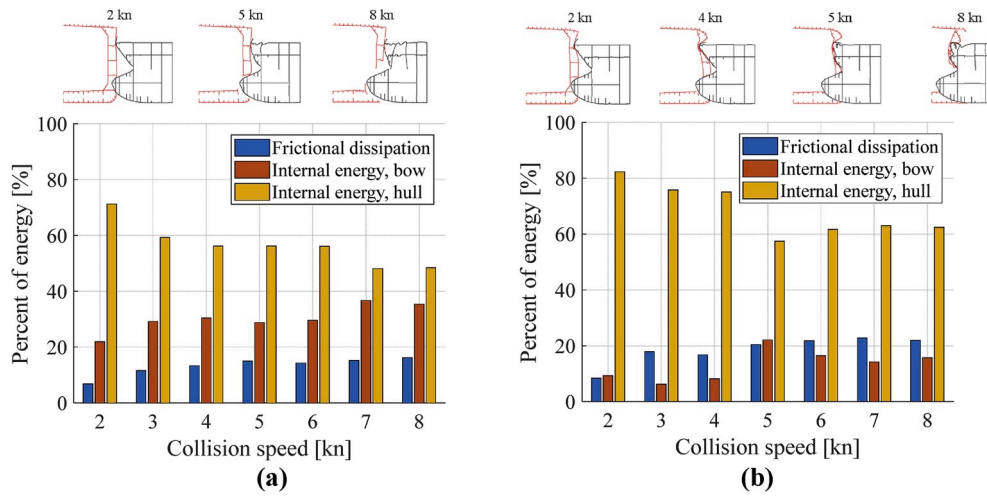
Fig. 10. Deformations and energy distributions from FEA of ship collisions: the struck ship is **(a)** non-corroded (T1) and **(b)** corroded (T5).

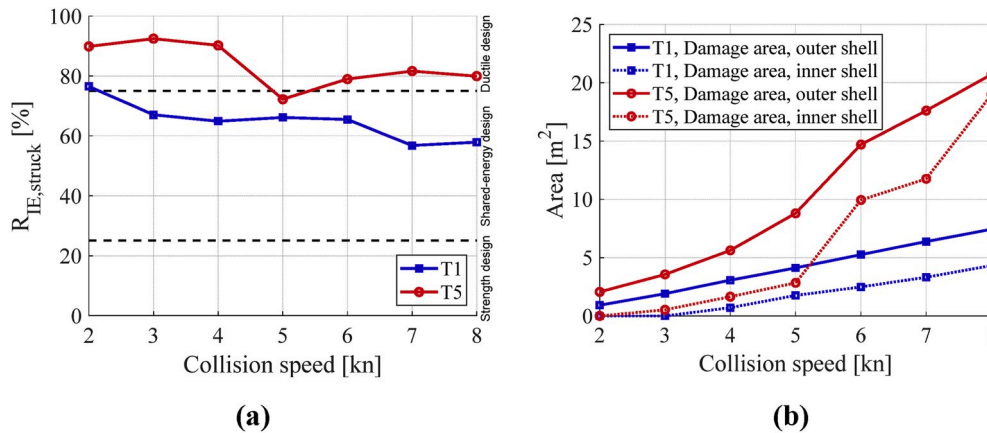**Fig. 11.** **(a)** Internal energy share ratio of the struck vessel, $R_{IE,struck}$, for different collision speeds and **(b)** projected damage opening areas in the struck ship's inner and outer side-shells.

270°, which corresponded to horizontal bending, biaxial bending, hogging and sagging conditions, respectively. Fig. 12 presents the bending moment-curvature diagrams and the longitudinal stress distributions at the maximum bending moment from FEA and the Smith method.

The difference between the methods in the predicted ultimate bending moment values was between 5% and 18% which is reasonably good. However, the predicted post-collapse behaviour varied to a larger degree. It was also found that the ULS was reached at a larger bending curvature and a higher bending moment in three of the four cases with the Smith model than with FEA. These differences may be explained by the definition of the LSE curves in the Smith method model, which were defined according to IACS (2019), where nonlinear behaviour of the structure elements was defined using the Ramberg-Osgood formula with a correction for plasticity. Since the elastic stiffness seemed to be less for the Smith model than for the FE model, the value of the curvature at the ULS should be higher for the former than for the latter.

Initial imperfections were implicitly incorporated in the formulae of LSE curves, while no geometrical distortions were introduced in the FE model. This should presumably lead to lower strength estimates, which is supported by the benchmark studies from Czujko et al. (2018) and Soares et al. (2008). Nevertheless, the Smith method applied in the current study generally overestimates ultimate strength compared to FEA. Similar trends were found in works by Parunov et al. (2018) and Tekgoz et al. (2018).

The selected approach for modelling a cross-section could be the source of variance in the results. For example, if elements at the intersection of plates are modelled as stiffened plates, their behaviour in compression will be affected by buckling. This will decrease the element's critical stress and the global strength of the hull. In contrast, if elements are assumed to act as hard corners instead, i.e., elastic-perfectly plastic, buckling will not be considered. In this case, the elastic limit will be reached at increased curvature values, the stiffness of the cross-section in the plastic region will increase, and the ULS will thus be affected.

Different sequences of failure modes predicted by the Smith method are another possible reason for the overestimation of bending strength. For example, the examination of the FEA results for hogging (90° loading direction) showed that bottom buckling is triggered first. According to the discussion above and the characteristics of the cross-section studied, double bottom and side plating consists of many hard corner elements. Due to the high stiffness of bottom plating, failure of the weather deck in yielding occurs prior to buckling of the double bottom. The yielding of elements in the upper part of the cross-section will force the NA to move downwards, resulting in a redistribution of the loads and postponing the occurrence of instability in the plating at the keel level.

The inclusion of hard corner elements is prescribed by CRS-H rules. In addition, interconnected plates fail mainly due to yielding in compression (IACS, 2019), since their stiffness is radically higher than
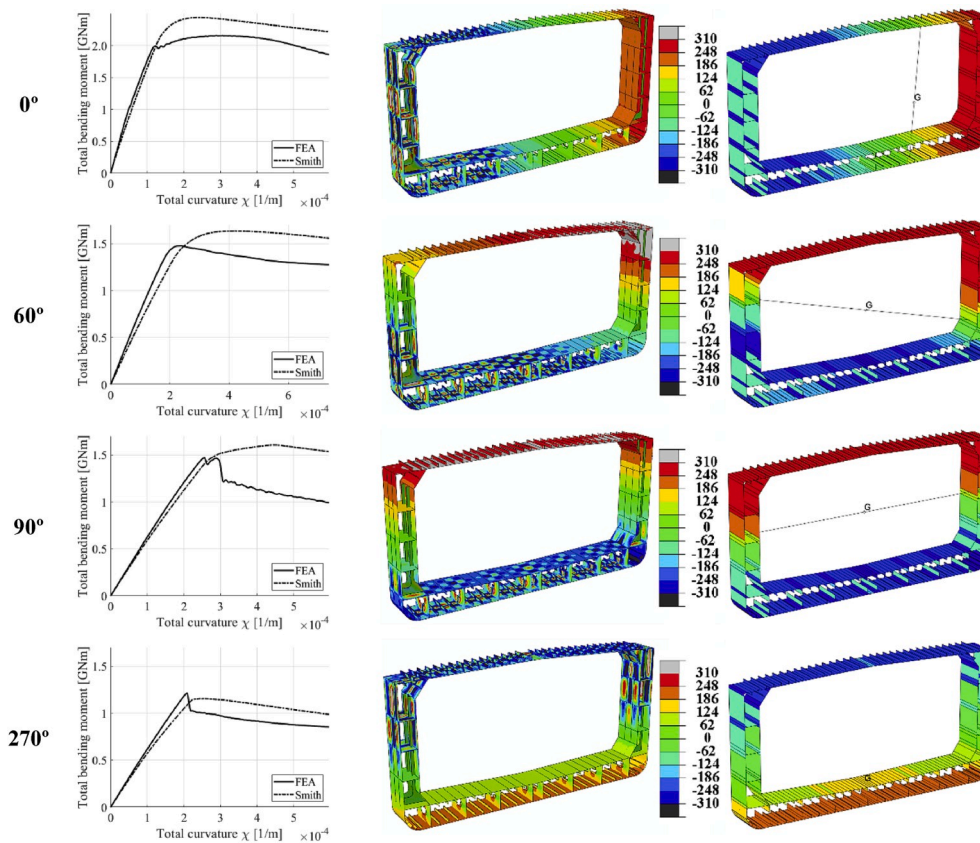
Fig. 12. (Left) Bending moment-curvature curves predicted using FEA and the Smith method, (middle) longitudinal stress distributions of FEA (results are presented for the critical section only), and (right) longitudinal stress distributions of the Smith method. The stresses are presented in [MPa].

the stiffness of an assembly of independent stiffened plate elements. Thus, despite the observed trends, it is believed that hard corners should be included in modelling for a realistic representation of a cross-section.

The longitudinal stress distributions in the cross-sections at ULS showed good agreement between FEA and the Smith method. The structural responses for both symmetric and asymmetric bending conditions agreed well. A comparison between the failure modes of the structures showed good agreement with the way distorted elements and their collapse modes occurred. The Smith method results showed the movement and rotation of the NA passing through the points in the cross-section with zero stresses. In conclusion, this initial comparison between the two methods showed that the FE model and Smith method model seemed to agree reasonably well.

4.2.2. Collision-damaged ship structure

The ship collision event was simulated according to Subsection 2.1 using the ship speed of 5 knots for the striking ship according to Sub-section 4.1. After the striking ship penetrated the mid-ship section of the struck vessel and reached zero knots, the bow of the striking ship was removed. The names of the FEA ship collision simulations are T1D for the non-corroded ship and T5D for the corroded ship (T5D). These simulations gave realistic shapes and sizes of the damage openings, as well as plastic deformations and failures of several structural elements. Fig. 13 presents the damage openings and equivalent plastic strains for T1D and T5D. In both cases, there was penetration through both of the side-shells and large plastic deformations of the structures. The structural damage was larger for T5D than for T1D because of the corroded material and reduced corrosion margins. The damage opening area was almost two times larger (see Fig. 11b), and the damage in the upper part near the weather deck was more prominent for T1D than for T5D. The outer plating was ruptured where the striking bow's forecastle impacted the struck ship. The internal longitudinals, transverse

stiffeners and bulkheads between plating were more severely distorted.

Using FEA, it was possible to continue with the ultimate strength analysis simulation according to the procedure presented in Subsection 2.2. However, it was not possible with the Smith method to represent damage openings, distorted structural elements or the plastic strain field in the same way. A study was therefore carried out to investigate how different degrees of simplification of collision-damaged structure modelling affect the ULS (see Fig. 14). The analyses were limited to hogging and sagging conditions. Five cases were defined for comparison:

- **Case A:** Full FEA where the ULS FEA was carried out by restarting the ship collision FEA after the struck vessel was removed.
- **Case B:** FEA where the FE model used in the ULS analysis had a damage opening shape and size corresponding to the projected damage area from the ship collision FEA. Note: only the shape and size of the damage opening were included; no other structural distortions, failures or plastic deformations were considered.
- **Case C:** FEA where the FE model used in the ULS analysis had a damage opening as defined in the Smith method model; see Section 3.
- **Case D:** FEA with the same FE model as in Case C, except that the material model was changed to the elastic-perfectly plastic material model used in the Smith method model.
- **Case E:** ULS analysis using the Smith method model.

Fig. 15 presents the results from the T1D and T5D ULS analyses for hogging and sagging conditions. For hogging, there was a large difference between Cases A and E i.e., the FEA and Smith method. There were minor differences between Cases B, C and D, which were between Cases A and E. The results for hogging for both T1D and T5D showed the importance of not simplifying the material and damage modelling with regards to 3 issues: (i) the damage opening area should not be simplified,
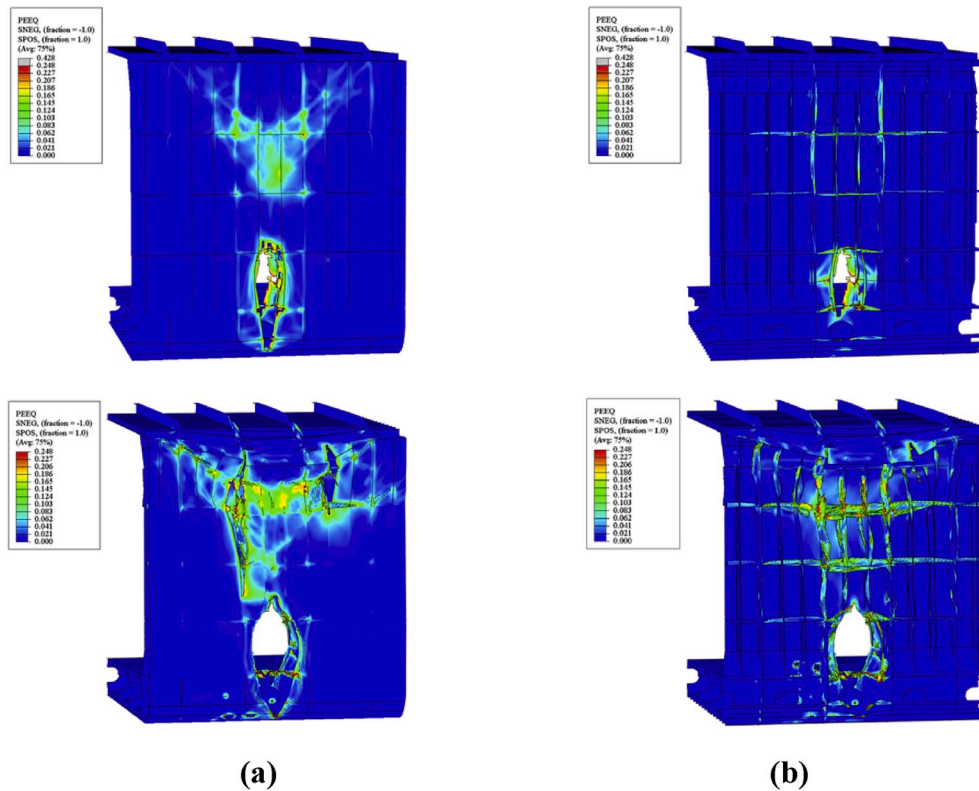
Fig. 13. Deformed and damaged side-shell structures after ship collision FEA.
The figures present the equivalent plastic strain (-
) according to von Mises **(a)** with and **(b)** without the outer shell plating for T1D (upper) and T5D (lower).
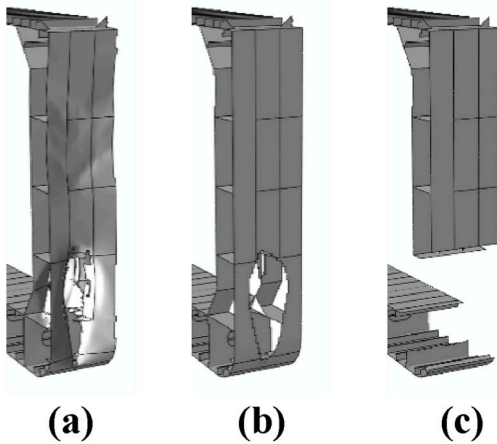
Fig. 14. Different collision damage models: **(a)** Case A, **(b)** Case B, and **(c)** Cases C, D and E. Note: only the mid-ship section is shown.

(ii) a realistic representation of the material's characteristics should be used, and (iii) deformed structures and plastic strains should not be disregarded.

The sagging results showed the same trend for Cases A, B and E as for hogging. However, Cases C and D showed larger ultimate bending moments than all the other cases. An analysis of the deformation of the FE ship model for these cases revealed that the simplified damage opening was the reason for these case results. The shape of the simplified damage opening delayed the failure modes of neighbouring structural elements and led to a higher ultimate bending moment compared in Cases C and D than in Cases A and B, which had a more realistic damage opening shape. Thus, these cases confirmed that simplified modelling of

collision-induced damage openings should be avoided in FE analysis.

Fig. 16 presents the results after the ultimate bending moments have been normalised by the corresponding Case A ultimate bending moment. The figure shows that all cases gave a high ultimate bending moment compared to the full FEA solution (Case A), which was recommended in this study. In the remaining part of the study, the Case A method was compared with the Case E method, i.e., full FEA and the Smith method, respectively. The results in Fig. 16 indicate that the Smith method overestimated the ultimate bending moments compared to FEA for hogging and sagging. The sizes of this overestimation under biaxial bending moment loading conditions are presented in Subsection 4.3.

4.3. Comparison of FEA and Smith method – biaxial bending moment loading conditions

#### 4.3.1. Ultimate strength analyses

The Smith method according to IACS (2019) is only applicable for pure vertical bending of undamaged ship structures. It does not consider rotation of the NA, and thus, the Smith method is not able to capture nonlinear structural collapse correctly for a ship structure subjected to biaxial bending. Fig. 17 presents the interaction curves of the ultimate bending moments during biaxial loading conditions from FEA and the Smith method proposed in this investigation; the Smith method in IACS (2019) is included for comparison but only for the T1I case in hogging and sagging conditions.

The results for the T1I case in Fig. 17a show that the tanker had a higher strength in the hogging condition than in the sagging condition because of the double bottom structure, which made a greater contribution than the single upper deck to the strength. The highest ultimate strength was found for pure horizontal bending, since the side-shell structures had a large distance to the centroid on the centerline, resulting in a high contribution to the moment of inertia. The results for
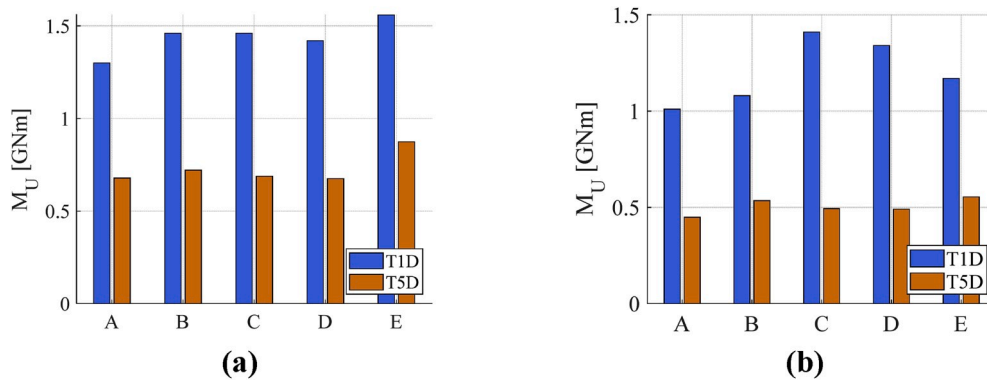
Fig. 15. Ultimate vertical bending moment for **(a)** hogging and **(b)** sagging loading conditions. The different cases compare FEA and the Smith method with regard to modelling the damage opening (see the text for details). Case A: full FEA; Case B: FEA without a deformed structure and plastic strains; Case C: FEA with a damage opening according to the Smith method model; Case D: the same FE model as in Case C but with elastic-perfectly plastic material; Case E: Smith method model.
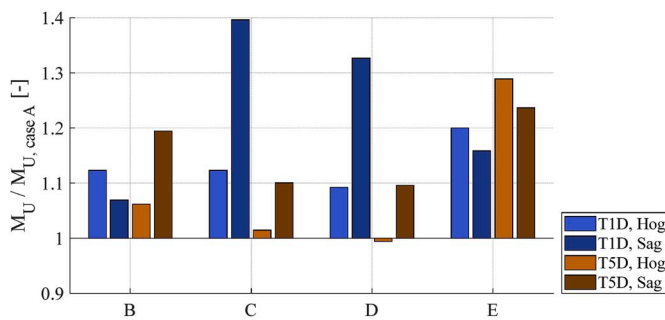
Fig. 16. Ultimate bending moments normalised by their corresponding ultimate bending moment in Case A.

the ultimate strength in vertical bending were identical for the Smith and CSR-H methods with differences of less than 1%. The discrepancies between the Smith method and FEA were 8% and 5% for hogging and sagging, respectively. Thus, the agreement between the three methods was considered to be good for pure vertical bending conditions. For all other loading combinations, the Smith method showed a larger ultimate strength than the FEA. The causes and reasoning in Subsection 4.2.1 also affected the other bending moment load combinations, but the short-comings of the Smith method resulted in a larger difference between the two methods. In addition, for the corroded ship structure case T5I shown in Fig. 17b, the trend was the same; the Smith method gave a slightly larger ultimate strength than the FEA. Notably, there was also a significant reduction in the ultimate strength capacity between T1I and T5I due to corrosion. The sagging condition was affected more than the hogging condition due to the large loss in hull strength in the upper deck; see Fig. 4b for the corrosion conditions.

Fig. 17c and d presents the results from the damaged ship structures with the damage opening on the port side of the ship. The largest reduction in ultimate strength for case T1D occurred in the second and third quadrants when the damaged side of the ship was in compression (see Fig. 8). The asymmetry was captured by both FEA and the Smith method. There was also a minor effect in the first and fourth quadrants compared to the T1I case, where the modelling of the damage opening showed a larger effect for FEA than for the Smith method model, as discussed in Subsection 4.2. For the corroded ship case T5D, there was a significant reduction in ultimate strength compared to T1D, where, as in the T5I case, there was a larger reduction in the sagging condition than in the hogging condition. Again, both methods captured the asymmetry due to the single-side damage opening. In contrast with the T1D case, the FEA results for T5D showed a large reduction in the first quadrant when the damaged side of the ship was in tension. An analysis of all FEAs showed that this can be explained by the damage and plastic

deformations caused by the forecastle, which led to a large reduction in strength, especially for these combinations of horizontal end bending moment loading conditions.

4.3.2. Residual strength index (RSI) calculation

The reserve strength of the case study ship was calculated in a residual strength analysis by the calculation of the RSI proposed by Fang and Das (2004). This was carried out for the three cases T1D, T5I and T5D for FEA and the Smith method, where T1I was the reference for both methods (see Fig. 18). The FEA results show a larger decrease than the Smith method results in RSI. For the T1D case, the difference can be explained by the simplification of the damage modelling in the Smith method (see Subsection 4.2), which can also be seen clearly in the asymmetric RSI results, which were better captured by FEA. For the corroded ship cases, there was a larger reduction in the RSI for FEA than for the Smith method. This can be explained by joint effects of too simplified damage and corrosion modelling in the Smith method, as found and discussed in the previous sections of this study.

4.4. Calibration method: FEA and Smith method

The results in the previous sections show that the FEA predicted lower ULS values for the biaxial bending moment loading conditions than the Smith method. However, each point on the FEA interaction curve took approximately 60 CPU hours to compute (see Section 3), while the entire interaction curve consisting of 35 points for the Smith method took 5 CPU minutes to calculate on the same computer. One of the advantages of using the FE method is the possibility of performing a detailed and accurate analysis of each specific load combination and "simulation scenario". However, if a high resolution of data points in the ULS interaction curve must be obtained, these analyses will be too demanding. Since the results in the previous sections showed that mostly the peak values of the ULS differed between the FEA and Smith methods, a "calibration" method using a curve fitting procedure was developed that makes use of as few FEAs as possible to generate correction factors for the main results of the Smith method.

A ULS interaction curve for an intact and non-corroded ship can be approximated by Equation (7) (Gordo and Soares, 1997), where M_y and M_z are coordinates on the "fitted" curve, M_{UH} and M_{UV} are the ultimate horizontal and vertical bending moments, respectively, and β is a shape factor, with $\beta = 2$ corresponding to an ellipse and $\beta > 1$ giving a shape similar to an ellipse:

$$\left(\frac{M_y}{M_{UV}}\right)^{\beta} + \left(\frac{M_z}{M_{UH}}\right)^{\beta} = 1 \tag{7}$$

For the damaged ship cases with asymmetric hull damage, the results in Subsection 4.3 showed that the ULS interaction curve was different in
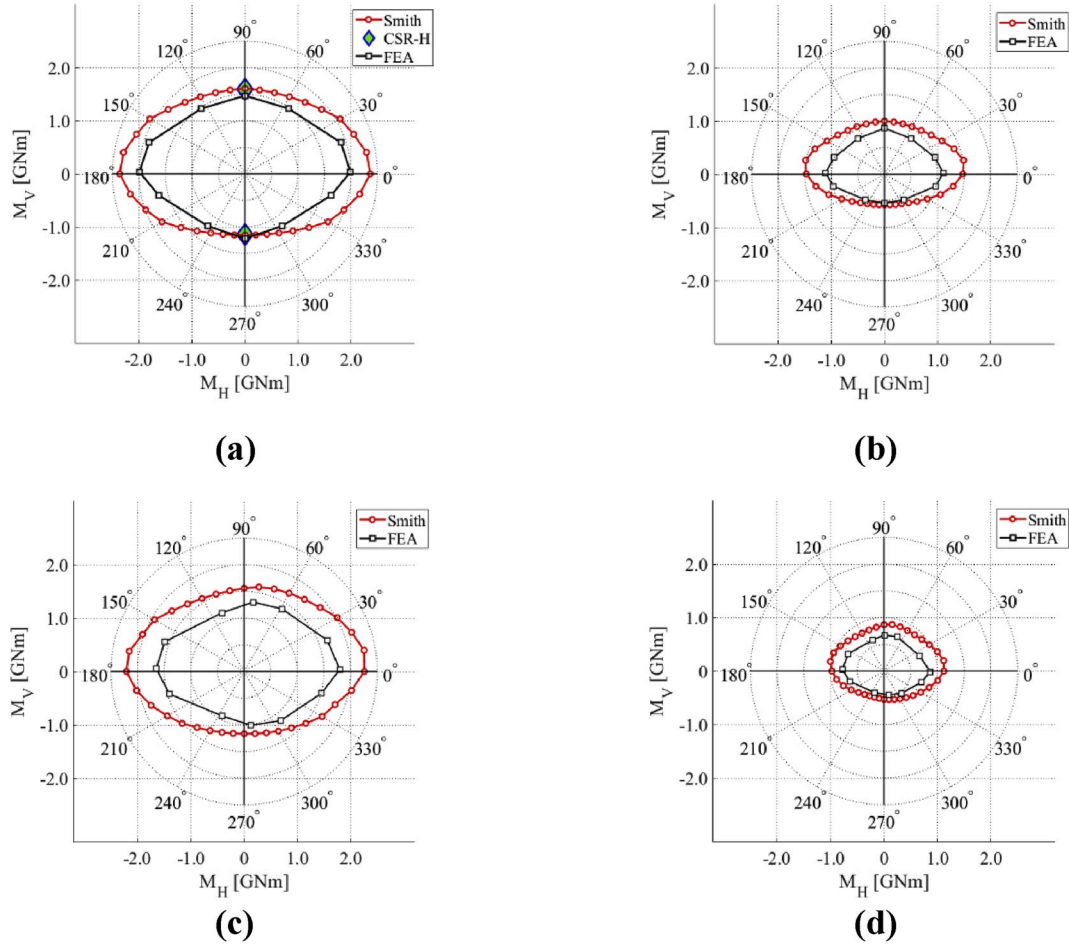
(a)

(b)

(c)

(d)

Fig. 17. ULS interaction diagrams of biaxial bending moment ratios for study cases **(a)** T1I, **(b)** T5I, **(c)** T1D, and **(d)** T5D.
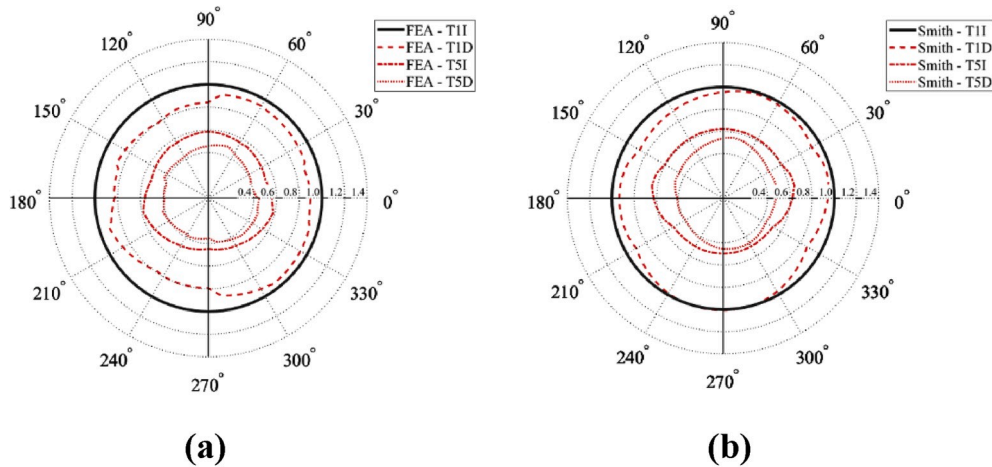

(a)

(b)

Fig. 18. RSI results from **(a)** FEA and **(b)** the Smith method.

all quadrants, especially when ship corrosion was also included. Thus, to generalise the calibration procedure, curve fitting was unique to each quadrant. It is recommended that at least four FEAs should be used for curve fitting in each quadrant to determine the shape factors; thus, in total, only 12 FEAs are needed, since pure vertical and horizontal bending can be shared points between quadrants. Note that for an intact structure, 7 points are sufficient due to symmetry around the vertical axis. Curve fitting was carried out by finding the solution with the lowest RMSE value between Equation (7) and the points obtained by FEA.

Based on the curves fitted using Equation (7) in each quadrant, both for FEA and the Smith method, calibration factors (*CF*) were calculated as the ratio between the two methods' fitted parameters. The *CFs* for pure horizontal and vertical ultimate bending moments were defined as $CF_H = M_{UH,FEA}/M_{UH,Smith}$ and $CF_V = M_{UV,FEA}/M_{UV,Smith}$, respectively. The *CF* for the shape factor was defined as $CF_\beta = \beta_{FEA}/\beta_{Smith}$. The new formulation of a "calibrated interaction curve" using the Smith method can then be described by Equation (8):

$$\left(\frac{M_y}{M_{UV,Smith}CF_V}\right)^{\beta_{Smith}CF_\beta} + \left(\frac{M_z}{M_{UH,Smith}CF_H}\right)^{\beta_{Smith}CF_\beta} = 1 \qquad (8)$$

Fig. 19 presents the results where calibration was performed for cases T1I, T5I, T1D and T5D. The results showed good agreement between the FEA and the Smith method with calibrated values according to Equation (8). Table 3 presents a summary of all curve-fitted parameters needed to plot the interaction curves using Equation (8). With the proposed procedure, which requires only a few FEA results together with the Smith method, a high-resolution interaction curve can be obtained with high confidence and rapidness compared to the time it takes to run many FEAs to obtain the same interaction curve resolution.
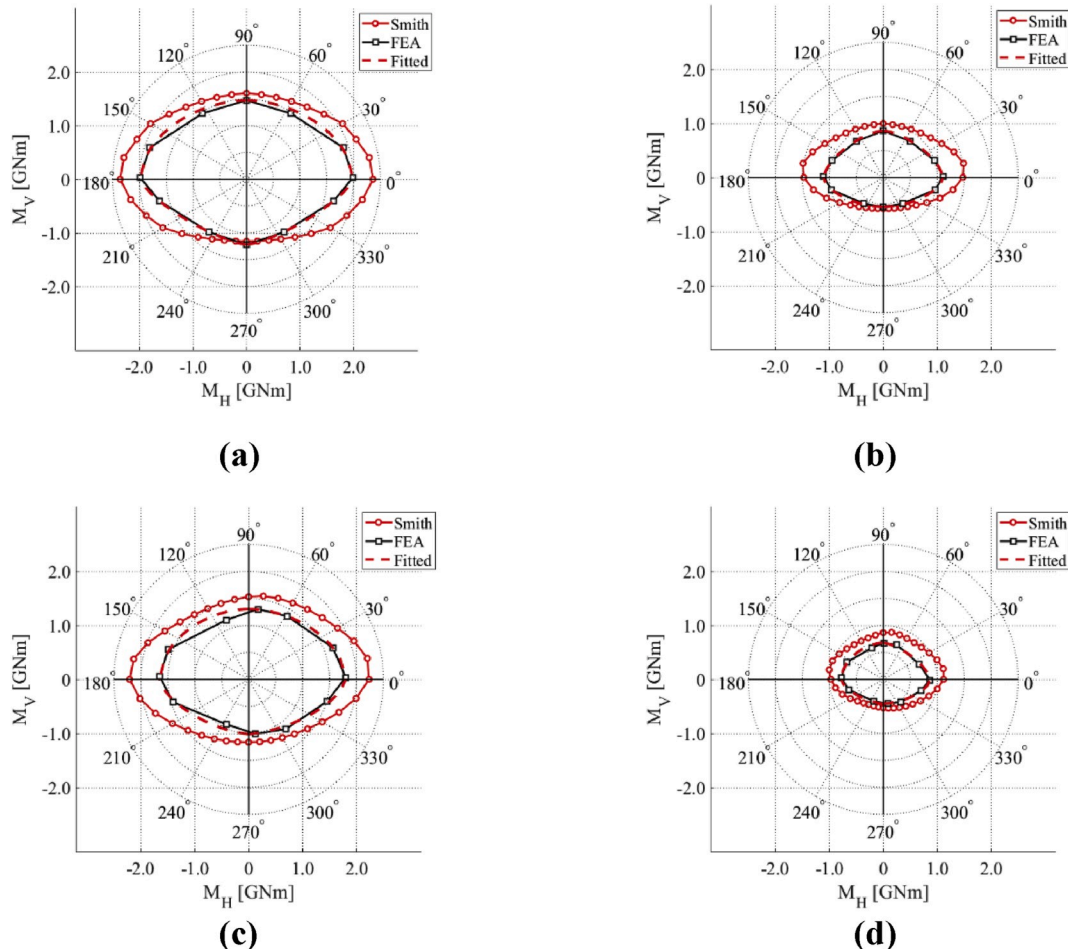
5. Conclusions

This study presented ultimate and residual strength analyses of a double-hull tanker ship during biaxial bending moment conditions. Two methods were compared: advanced nonlinear FE analyses and the Smith method according to Fujikubo et al. (2012). The case study vessel was analysed from the perspective of an intact hull and a hull damaged due to ship collision under two physical conditions: newly built (non-corroded) and aged due to corrosion.

The results for the non-corroded and intact ship hull structures showed good agreement between the FEA, the Smith method and IACS CSR-H for vertical bending loading conditions. For all other load combinations, the ultimate bending moments were always lower for the FEA than for the Smith method. It was found that this discrepancy was related to how the material modelling in the Smith method was proposed in the IACS (2019) procedures. For corroded and intact ship hull

Table 3

Curve-fitted parameters to the "calibrated" Smith method according to Equation (8); "Qi" indicates quadrant number (i = 1, 2, 3 or 4).

Case	Parameter	Q1	Q2	Q3	Q4
T1I	$M_{UH,\ Smith}$; $M_{UV,Smith}$ [GNm]	2.36; 1.61	−2.36; 1.61	−2.36; −1.15	2.36; −1.15
	β	1.91	1.91	1.95	1.95
	CF_H; CF_V	0.84; 0.97	0.84; 0.92	0.84; 1.06	0.84; 1.06
	CF_β	0.97	0.97	0.68	0.68
T5I	$M_{UH,\ Smith}$; $M_{UV,Smith}$ [GNm]	1.49; 1.00	−1.49; 1.00	−1.48; −0.57	1.48; −0.57
	β	1.76	1.76	1.82	1.82
	CF_H; CF_V	0.75; 0.87	0.75; 0.87	0.75; 0.95	0.75; 0.95
	CF_β	0.85	0.85	0.93	0.93
T1D	$M_{UH,\ Smith}$; $M_{UV,Smith}$ [GNm]	2.23; 1.54	−2.21; 1.53	−2.21; −1.16	2.23; −1.16
	β	1.91	1.62	1.73	1.58
	CF_H; CF_V	0.81; 0.84	0.75; 0.84	0.75; 0.87	0.81; 0.87
	CF_β	0.97	1.17	0.88	0.99
T5D	$M_{UH,\ Smith}$; $M_{UV,Smith}$ [GNm]	1.12; 0.87	−1.00; 0.87	−0.97; −0.53	1.12; −0.53
	β	1.78	1.68	1.58	1.78
	CF_H; CF_V	0.77; 0.78	0.78; 0.78	0.80; 0.85	0.77; 0.84
	CF_β	0.82	1.07	0.97	0.95

(a)

(b)

(c)

(d)

Fig. 19. Interaction curves for FEA, the Smith method and the Smith method corrected according to Equation (8) for **(a)** T1I, **(b)** T5I, **(c)** T1D, and **(d)** T5D.

structures, the difference was larger, which was also found to be due to the simplified material modelling in the Smith method model.

Prior to ULS analyses of the collision-damaged hull structures, a sensitivity study on the ultimate strength in hogging and sagging conditions due to various accepted simplifications during the modelling of hull damage was performed. It was found that the Smith method, because of restrictions and the possibility to model hull damage, overestimated the ULS compared to FEA, which was considered more trustworthy and realistic. Hence, the Smith method resulted in unconservative results for safe ship design with respect to ultimate strength. The cause of this result was found to be related to three issues, which resulted in three recommendations: (i) the shape and size of the damage opening should not be simplified to simplistic shapes; (ii) a representative constitutive material model for the material's true characteristics should be used; and (iii) deformed structures and plastic strains should not be disregarded.

The results from ultimate strength analyses of the collision-damaged ship structures showed that both FEA and the Smith method captured the expected asymmetric response in ultimate strength due to asymmetric damage. The RSI calculation showed that the reduction was larger for FEA than for the Smith method and was often the largest for biaxial bending moment loadings than for pure vertical bending moment conditions. This showed the importance of calibrating the Smith method for ULS analyses for biaxial bending moment conditions. A procedure for such a calibration, combining the results from a few FEAs and the advantages of the Smith method, was proposed. With this procedure, the advantages of detailed FEA for damaged ship structure and corrosion are improvements compared to the simplifications made using the Smith method alone. The proposal also gives a safe ship design procedure with ultimate strength bending moments that are not overestimated due to model simplifications or other errors.

Declaration of competing interest

The authors declare that they have no known competing financial interests or personal relationships that could have appeared to influence the work reported in this paper.

CRediT authorship contribution statement

Artjoms Kuznecovs: Conceptualization, Methodology, Software, Formal analysis, Writing - original draft, Visualization. **Jonas W. Ringsberg:** Conceptualization, Methodology, Formal analysis, Writing - original draft, Supervision, Project administration, Funding acquisition. **Erland Johnson:** Conceptualization, Methodology, Formal analysis, Writing - review & editing, Supervision. **Yasuhira Yamada:** Methodology, Formal analysis, Writing - review & editing.

Acknowledgements

References

AbuBakar, A., Dow, R.S., 2013. Simulation of ship grounding damage using the finite element method. Int. J. Solid Struct. 50 (1), 623–636.

Campanile, A., Piscopo, V., Scamardella, A., 2015. Statistical properties of bulk carrier residual strength. Ocean Eng. 106 (1), 47–67.

Choung, J., Nam, J.M., Ha, T.B., 2012. Assessment of residual ultimate strength of an asymmetrically damaged tanker considering rotational and translational shifts of neutral axis plane. Mar. Struct. 25 (1), 71–84.

Czujko, J., Bayatfar, A., Smith, M., et al., 2018. Technical committee III.1 - ultimate strength. In: Kaminski, M.L., Rigo, P. (Eds.), Proceedings of the 20th International Ship and Offshore Structures Congress ISSC2018, vol. 1. IOS Press, Amsterdam, The Netherlands, pp. 335–439. Liege, Belgium/Amsterdam, the Netherlands.

Ehlers, S., 2010. The influence of the material relation on the accuracy of collision simulations. Mar. Struct. 23 (4), 462–474.

Ehlers, S., Østby, E., 2012. Increased crashworthiness due to arctic conditions – the influence of sub-zero temperature. Mar. Struct. 28 (1), 86–100.

Faisal, M., Noh, S.H., Kawsar, M.R.U., Youssef, S.A.M., Seo, J.K., Ha, Y.C., Paik, J.K., 2016. Rapid hull collapse strength calculations of double hull oil tankers after collisions. Ships Offshore Struct. 12 (5), 624–639.

Fang, C., Das, P.K., 2004. Hull girder ultimate strength of damaged ships. In: Proceedings of the 9th Symposium on Practical Design of Ships and Other Floating Structures (PRADS 2004). Lübeck-Travemuende, Germany, pp. 309–316.

Fujikubo, M., Takemura, K., Oka, S., Alie, M.Z.M., Iijima, K., 2012. Residual hull girder strength of asymmetrically damaged ships. J. Jpn. Soc. Nav. Archit. Ocean Eng. 16 (1), 131–140.

Garbatov, Y., Soares, C.G., Parunov, J., Kodvanj, J., 2014. Tensile strength assessment of corroded small scale specimens. Corrosion Sci. 85 (1), 296–303.

Garbatov, Y., Parunov, J., Kodvanj, J., Saad-Eldeen, S., Soares, C.G., 2016. Experimental assessment of tensile strength of corroded steel specimens subjected to sandblast and sandpaper cleaning. Mar. Struct. 49 (1), 18–30.

Gordo, J.M., Soares, C.G., 1997. Interaction equation for the collapse of tankers and containerships under combined bending moments. J. Ship Res. 41 (3), 230–240.

Hogström, P., Ringsberg, J.W., 2012. An extensive study of a ship's survivability after collision – a parameter study of material characteristics, non-linear FEA and damage stability analyses. Mar. Struct. 27 (1), 1–28.

Hogström, P., Ringsberg, J.W., 2013. Assessment of the crashworthiness of a selection of innovative ship structures. Ocean Eng. 59 (1), 58–72.

Hogström, P., Ringsberg, J.W., Johnson, E., 2009. An experimental and numerical study of the effects of length scale and strain state on the necking and fracture behaviours in sheet metals. Int. J. Impact Eng. 36 (10–11), 1194–1203.

Hussein, A.W., Soares, C.G., 2009. Reliability and residual strength of double hull tankers designed according to the new IACS Common Structural Rules. Ocean Eng. 36 (17–18), 1446–1459.

IACS, 2019. Common structural rules for bulk carriers and oil tankers. Available online [accessed: 2020-02-20]. http://www.iacs.org.uk/publications/common-structural -rules/csr-for-bulk-carriers-and-oil-tankers/.

IMO, 2010. Resolution MSC.287 - adoption of the international goal-based ship construction Standards for bulk carriers and oil tankers. Available online [accessed: 2020-02-20]. http://www.imo.org.

Kuznecovs, A., Shafieisabet, R., 2017. Analysis of the Ultimate Limit State of Corroded Ships after collision. MSc Thesis Report X-17/376. Chalmers University of Technology, Gothenburg, Sweden.

Makouei, S.H., Teixeira, A.P., Soares, C.G., 2015. A study on the progressive collapse behaviour of a damaged hull girder. In: Soares, C.G., Santos, T.A. (Eds.), Proceedings of the International Conference Maritime Technology and Engineering (MARTECH 2015), Lisbon, Portugal. Taylor & Francis Group, London, UK, pp. 405–416.

Marinatos, J.N., Samuelides, M.S., 2015. Towards a unified methodology for the simulation of rupture in collision and grounding of ships. Mar. Struct. 42 (1), 1–32.

NORSOK, 2004. NORSOK Standard - Design of Steel Structures, N-004. Available online [accessed: 2020-02-20]. https://www.standard.no/pagefiles/1145/n-004.pdf.

Paik, J.K., 2018. Ultimate Limit State Analysis and Design of Plated Structures, second ed. Wiley-Blackwell, Hoboken, New Jersey, USA.

Paik, J.K., Melchers, R.E., 2008. Condition Assessment of Aged Structures, first ed. CRC Press, Cambridge, UK.

Paik, J.K., Lee, J.M., Hwang, J.S., Park, Y.I., 2003a. A time-dependent corrosion wastage model for the structures of single- and double-hull tankers and FSOs and FPSOs. Mar. Technol. 40 (3), 201–217.

Paik, J.K., Lee, J.M., Park, Y.I., Hwang, J.S., Kim, C.W., 2003b. Time-variant ultimate longitudinal strength of corroded bulk carriers. Mar. Struct. 16 (8), 567–600.

Paik, J.K., Kim, B.J., Seo, J.K., 2008a. Methods for ultimate limit state assessment of ships and ship-shaped offshore structures: Part III hull girders. Ocean Eng. 35 (2), 281–286.

Paik, J.K., Thayamballi, A.K., Melchers, R.E., 2008b. Some recent developments in corrosion assessment and management for steel ships and offshore structures. Mar. Technol. SNAME News 45 (2), 94–100.

Parunov, J., Rudan, S., Gledić, I., Primorac, B.B., 2018. Finite element study of residual ultimate strength of a double hull oil tanker with simplified collision damage and subjected to bi-axial bending. Ships Offshore Struct. 13 (S1), S25–S36.

Ringsberg, J.W., Li, Z., Johnson, E., 2017. Performance assessment of the crashworthiness of corroded ship hulls. In: Soares, C.G., Garbatov, Y. (Eds.), Progress in the Analysis and Design of Marine Structures - Proceedings of the 6th International Conference on Marine Structures (MARSTRUCT 2017), Lisbon, Portugal. Taylor & Francis Group, London, UK, pp. 523–531.

Ringsberg, J.W., Li, Z., Johnson, E., Kuznecovs, A., Shafieisabet, R., 2018a. Reduction in ultimate strength capacity of corroded ships involved in collision accidents. Ships Offshore Struct. 13 (S1), S155–S166.

Ringsberg, J.W., Li, Z., Kuznecovs, A., Johnson, E., 2018b. Analysis of the ultimate strength of corroded ships involved in collision accidents and subjected to biaxial bending. In: Soares, C.G., Santos, T.A. (Eds.), Progress in Maritime Technology and Engineering - Proceedings of the 4th International Conference on Maritime Technology and Engineering (MARTECH 2018), Lisbon, Portugal. Taylor & Francis Group, London, UK, pp. 327–336.

Saad-Eldeen, S., Garbatov, Y., Soares, C.G., 2011. Experimental assessment of the ultimate strength of a box girder subjected to severe corrosion. Mar. Struct. 24 (4), 338–357.

Samuelides, M., 2015. Recent advances and future trends in structural crashworthiness of ship structures subjected to impact loads. Ships Offshore Struct. 10 (5), 488–497.

Smith, C.S., 1977. Influence of local compressive failure on ultimate longitudinal strength of a ship's hull. In: Proceedings of the 3rd International Symposium on Practical Design in Shipbuilding. PRADS 1977), Tokyo, Japan, pp. 73–79.

Smith, M.J., Pegg, N.G., 2003. Automated assessment of ultimate hull girder strength. J. Offshore Mech. Arctic Eng. 125 (3), 211–218.

Soares, C.G., Luis, R.M., Nikolov, P., et al., 2008. Benchmark study on the use of simplified structural codes to predict the ultimate strength of a damaged ship hull. Int. Shipbuild. Prog. 55 (1–2), 87–107.

Storheim, M., Alsos, H.S., Hopperstad, O.S., Amdahl, J., 2015. A damage-based failure model for coarsely meshed shell structures. Int. J. Impact Eng. 83 (1), 59–75.

Systèmes, Dassault, 2020. Abaqus unified FEA. Available online [accessed: 2020-02-20]. https://www.3ds.com/products-services/simulia/products/abaqus/.

Tekgoz, M., Garbatov, Y., Soares, C.G., 2018. Strength assessment of an intact and damaged container ship subjected to asymmetrical bending loadings. Mar. Struct. 58 (1), 172–198.

Yamada, Y., 2014. Numerical study on the residual ultimate strength of hull girder of a bulk carrier after ship-ship collision. In: Proceedings of the ASME 2014 33rd International Conference on Ocean, Offshore and Arctic Engineering (OMAE 2014), p. 11. San Francisco, CA, USA. Paper No. OMAE2014-23811, V04AT02A061.

Yamada, Y., 2019. Dynamic collapse mechanism of global hull girder of container ships subjected to hogging moment. J. Offshore Mech. Arctic Eng. 141 (5), 051605, 15 pages.

Yamada, Y., Ogawa, Y., 2011. Study on the residual ultimate longitudinal strength of hull girder of a bulk carrier against a sagging moment after ship collision. In: Soares, C. G., Fricke, W. (Eds.), Advances in Marine Structures - Proceedings of the 3rd International Conference on Marine Structures (MARSTRUCT 2011), Hamburg, Germany. Taylor & Francis Group, London, UK, pp. 429–436.

Zhang, S., Pedersen, P.T., 2017. A method for ship collision damage and energy absorption analysis and its validation. Ships Offshore Struct. 12 (S1), S11–S20.